

Gas sensors based on nanostructures of semiconductors ZnO and TiO₂

T. PUSTELNY^{1*}, M. PROCEK¹, E. MACIAK¹, A. STOLARCZYK², S. DREWNIAK¹,
M. URBAŃCZYK¹, M. SETKIEWICZ¹, K. GUT¹, and Z. OPILSKI¹

¹ Department of Optoelectronics, Silesian University of Technology, 2 Akademicka St., 44-100 Gliwice, Poland

² Department of Physical Chemistry and Technology of Polymers, Silesian University of Technology, 9 Strzody St., 44-100 Gliwice, Poland

Abstract. The paper presents a resistance structures with sensor layers based on nanostructures elaborated on the base of TiO₂ and ZnO. The structures were tested concerning their sensitivities to the effects of nitrogen dioxide in the atmosphere of synthetic air. The TiO₂ and ZnO nanostructures played the role of sensor layers. Investigations have proved that the elaborated resistance structures with TiO₂ and ZnO layers are sensitive to the presence of NO₂ in the atmosphere of synthetic air. The resistance of the structure amounted to about 20Ω in the case of ZnO structures and to about 200Ω in the case of TiO₂ structures. The investigations confirmed that resistance structures with ZnO and TiO₂, exposed to the effect of nitrogen dioxide in the atmosphere of synthetic air changes their resistances relatively fast. This indicates that such structures might be practically applied in sensors of nitrogen dioxide ensuring a short time of response.

Key words: gas sensors, nanostructures, TiO₂, ZnO.

1. Introduction

Recently, more and more attention has been devoted to monitoring the quality of air [1] and environment [2] and to the detection of war gases and explosives by detecting their vapours [3, 4]. In 2005 the Kyoto Treaty came into force, concerning the constraint of the emission of some gases (including – nitrogen oxides) into the atmosphere in order to restrict the greenhouse effect [5]. In all systems of monitoring and detecting gases extremely sensitive gas sensors should be applied permitting the detection and determination of weak concentrations on the level of single ppm (parts per million) and even ppb (parts per billion) in the atmosphere of air. Such gas sensors are also applied in medical diagnostics [6], chemical industry, food industry and other domains.

Nitrogen oxides (NO_x) constitute an important group of toxic gases whose concentration in the air ought to be controlled due to their considerable pernicious effects. Nitric compounds are also components of the vapours of such explosives as TNT, RDX and nitroglycerin [3]. An important group of sensors which proved to be effective in the determination of the concentration and the detection of NO_x are sensors based on semiconductors with a wide forbidden energy gap, including metal oxides, such as TiO₂ [7], SnO₂ [8], WO₃ [9], In₂O₃, ZnO [10], Fe₂O₃ and combination of those semiconductors. Sensors based on these materials (semiconductors) can be applied in various types of gas sensors, among others in resistance sensors, optical sensors, sensors with a surface acoustic wave and QCM (quartz crystal microbalance) sensors [11–15].

Titanium dioxide (TiO₂) has been applied already for many years in photo- and electrochemical systems (e.g. in

photocatalysis and in solar cells [16]). Attempts have been made to apply TiO₂ for the detection of gases, including: NH₃ [17], CO [18], H₂ [19], H₂S [20], vapours of alcohols [21], humidity [22] and others.

A well-known and widely applied material is also zinc oxide (ZnO) [18]. In recent years the application of ZnO has been widely investigated due to its piezoelectric, optoelectronic, acoustoelectronic and sensoric properties [16, 21].

In the domain of gas sensors the most often resistance sensors are used, operating thanks to electrical conductance changes of the semiconductor caused by the adsorption of atoms and molecules on its surface. In resistance sensors semiconductors with a wide energy band display considerable possibilities of measuring because their sensoric properties can be modified by adequate doping. Gas sensors based on such kind semiconductors require, however an elevated temperature of operation typical within the range of 200–400°C, or their activation by means of UV radiation [16].

In every kind of gas sensors the most important problem is the adequate choice of the sorbent – the material which permits to scan the change of signals caused by changes of the concentration of the gas detected in the gas-carrier atmosphere. The best known and widely applied sensors are thin-layer ones, obtained in various ways, e.g. by vacuum sputtering, by an electron beam, magnetron sputtering, deposition from the solution etc. Besides that also the effect of various admixtures of transition metals is known, which improves the sensitivity and selectivity of these sensors. The sensitivity of thin-layer sensors depends on the area of the sorbent surface affected by the molecules of the gas which is to be detected. The metrology requires a continuous increasing

*e-mail: Tadeusz.Pustelny@polsl.pl

of the sensitivity and decreasing response time of the sensors at simultaneously reduction of their dimensions and consumption of energy. This can be achieved by influencing properly the morphology and topology of the surface of the adsorbing element. In recent years much interest has been devoted to nano- and microparticles forming a developed sorption structure, the surface area of which is much larger than that of thin layers. Various methods of obtaining nanoparticles of TiO_2 and ZnO have been developed, among them the hydrothermal method, the sol-gel method, the chemical vapour deposition (CVD) method and solution grown method [23–25].

The paper presents the results of investigations concerning resistance sensors based on nanoparticles of ZnO and TiO_2 , viz. nanorods, nanotubes, nanobelts, as well as complex nanostructures. Further on the methods of synthesizing such nanostructures are presented, and also the results of investigations concerning gas sensors constructed by their applications.

2. Syntheses of sensoric nanostructures

2.1. Nanotubes and nanobars of ZnO . In technological processes the following materials were used: $\text{Zn}(\text{NO}_3)_2 \cdot 6\text{H}_2\text{O}$ (produced by POCH Gliwice), NaOH (produced by POCH), ethylenediamine EDA (produced by Fluka) and ethanol (produced by Aldrich). In order to obtain various morphologies two syntheses were performed:

Synthesis A: In a teflon vessel 0.600 g NaOH and 0.440 g $\text{Zn}(\text{NO}_3)_2 \cdot 6\text{H}_2\text{O}$ were solved in 3 ml of deionized water (at the ratio of Zn^{+2} ions to OH^- ions equal to 1:10). Then 30 ml ethanol, 5 ml deionized water and 5 ml EDA were added. The solution was placed for 30 minutes in an ultrasonic bath and next passed to an autoclave. The reaction was run at a temperature of 180°C for two hours. After the reaction in the autoclave had been cooled down, the obtained sediment was centrifuged, repeatedly rinsed in deionized water and ethanol. The zinc oxide was dried for 12 hours under reduced pressure (15 mbar) at room temperature.

Synthesis B: The process was similar to that of synthesis A, but at different ratio of the base, viz. 1.2 g NaOH (ratio of the ions Zn^{+2} : OH^- equal to 1:20) and the mixture was kept longer in the ultrasonic bath (40 minutes).

After the syntheses the obtained structures were depicted by means of a scanning electron microscope (SEM) SUPRA 35, produced by ZEISS. As is to be seen in Fig. 1, in result of these syntheses two different morphologies of ZnO were achieved. These are, respectively, nanotubes with various dimensions (synthesis A) and flower-shaped agglomerates of nanowires (synthesis B). It has been perceived that in synthesis B the obtained structures are more homogeneous, i.e. agglomerates with a diameter of several μm . The effect of synthesis A is a mixture of nanotubes with various dimensions and granules with a diameter of several score to several hundreds nm.

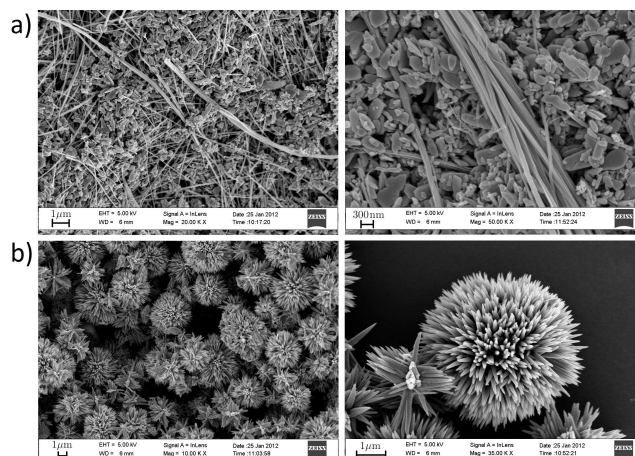


Fig. 1. SEM images of ZnO nanoparticles made in: a) synthesis A; b) synthesis B

2.2. TiO_2 nanoparticles. Nanofibres of TiO_2 were obtained by means of the hydrothermal method [24]. For this purpose the following materials were used: anatase (produced by Sigma Aldrich), KOH (produced by POCH, Gliwice, Poland), ethanol (also produced by POCH) and deionized water.

Into a teflon vessel 0.5 g anatase and 20 ml of 10-mole sodium hydroxide solution were introduced. The suspension had been stirred for 10 minutes at room temperature and then passed into the autoclave. The reaction was run for 72 hours at temperature of 150°C , stirring the mixture all the time. After its removal from the autoclave the sediment was decanted, repeatedly rinsed with deionized water and next with 0.1 mol HCl solutions until an acid reaction of the filtrate was achieved. The residual hydrochloric acid was rinsed in deionized water until a chemically inert pH was reached. The resulting titanium acid IV was passed into a quartz crucible, preliminarily dried for one hour at a temperature of 70°C . Then the titanium acid was divided into three batches and again subjected for one hour to thermal calcinations treatment at various temperature viz. 350°C (TiO_2 350), 450°C (TiO_2 450) and 550°C .

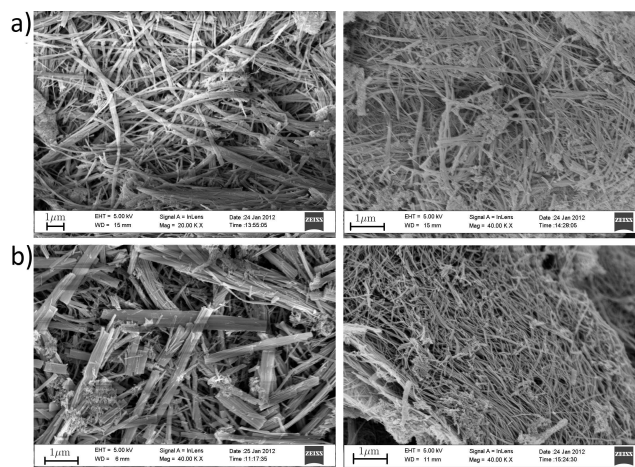


Fig. 2. SEM images of the TiO_2 nanoparticles: a) left calcined in 350°C ; right calcined in 450°C ; b) calcined in 550°C from different areas

Similarly as in the case of ZnO, the obtained structures were depicted by means of SEM and presented in Fig. 2. These images indicate that the temperature of calcination influences the length and homogeneity of the obtained fibers.

3. Investigations of TiO₂ and ZnO structures by optical methods

ZnO and TiO₂ nanostructures have both been chemically checked making use of the Raman spectroscopy. The Raman spectra are presented in Fig. 3. This permitted to determine the purity of the structures and to check their crystallization quality. The obtained nanoparticles of TiO₂ have a

form of anatase which was confirmed by the Raman spectroscopy study [26]. The obtained structures have been illustrated by means of confocal microscopy and scanning Raman microscopy (in the investigations the NTEGRA Spectra NT-MDT with excitation by green laser of 532 nm was applied). The results of this illustrating are shown in Fig. 4. Both images of the given samples were obtained simultaneously using the same laser beam in the same spot of the sample. The images have a resolution of 256 × 256 points with smoothing. The Raman presentations were performed basing on the field under the given peak (for Raman sifts: ZnO – 553 cm⁻¹ and TiO₂ – 640 cm⁻¹).

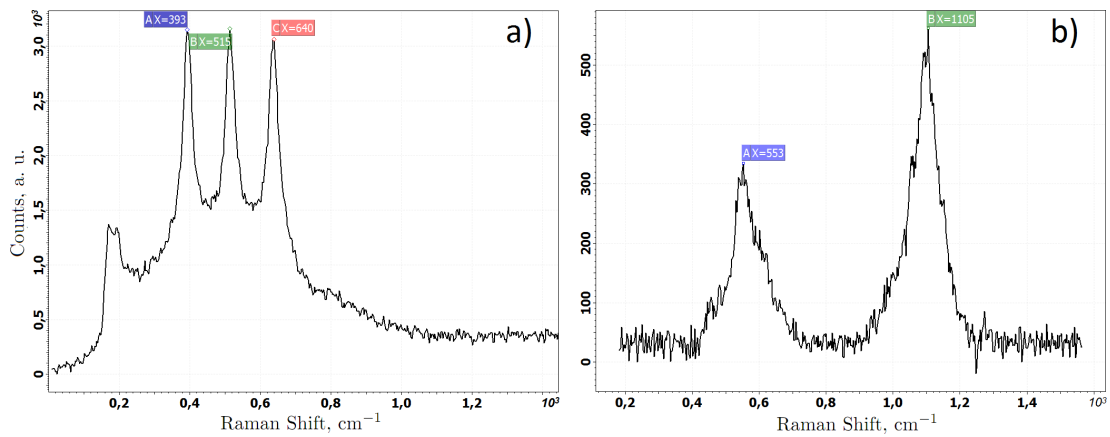


Fig. 3. Examples of Raman spectra of: a) TiO₂ nanostructures calcined at temperature 450°C; b) ZnO made according to synthesis A

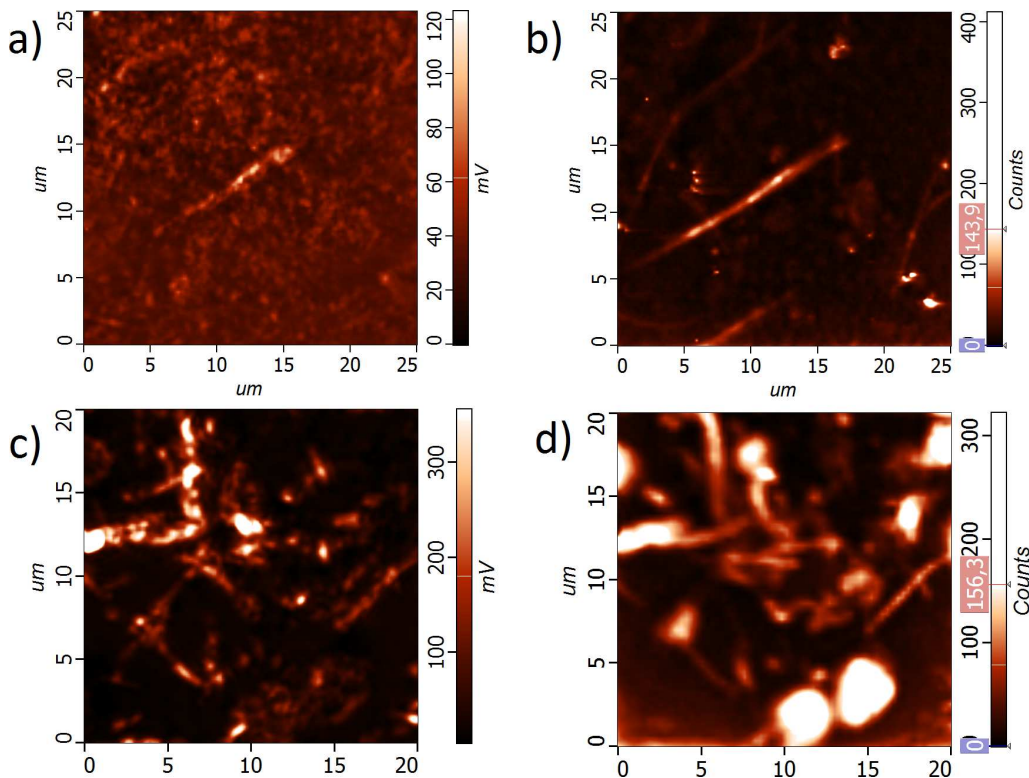


Fig. 4. Optical imaging of structures of ZnO and TiO₂, a) confocal microscopy image of ZnO A, b) Raman mapping image of ZnO A, c) confocal microscopy image of TiO₂ 350, d) Raman mapping of TiO₂ 350. (Images was created using NTEGRA Spectra NT-MDT system with 532 nm laser)

The resolution of the images of confocal microscopy is perceptively worse than in the case of Raman mapping. While in confocal images only the outlines of nanofibres are visible, in the Raman images distinct needles can be seen, particularly in the case of ZnO obtained by means of synthesis A, where single fibers could be illustrated. TiO₂ maps are somewhat worse, because agglomerate was tested causing lessens of the contrast due to the higher chemical homogeneity. More it becomes obvious that diffractive restrictions permit in the case of confocal images to perceive only the outlines of the shape. What is more, a confocal image does not provide information about the chemical composition. Raman images are more distinct thanks to the greater contrast between the background, lacking the investigated wavelength, and the element which due to the Raman scattering emits the given wavelength. Basing on the Raman mapping we may try to assess the dimensions of the fibers. In the case of such small structures, however, SEM (Scanning Electron Microscopy) proves to be more adequate because there are no restrictions of diffraction in this range of dimensions. Attempts have also been made to apply a atomic force microscopy (AFM) for the purpose of investigating such structures. Unfortunately, the rather weak adhesion of the materials to the substrate and the strong polarity (particularly of TiO₂) make measurements impossible without the application of some binding agent, because the nanoparticles stick to the cantilever and tip.

4. Sensor performance

Transducer system is a four comb electrode array with period of 10 μm. It was made of gold in photolithographic lift-off process on glass substrate with dimensions 20 × 30 mm. The way of constructing a similar transducer, though made on silicon substrate, and its characteristics have been described in [26]. The sorbets were deposited dropwise. The previously prepared nanoparticles were dispersed in pure ethanol (produced by POCH) stirring it for 15 minutes using for this purpose a magnetic mixer until a homogeneous suspension was achieved. In the process of depositing the sorbets on the plate with the transducers to the plate was attached by means of a neodymium magnet the mask, so that only the required areas were covered with the sorbent. Immediately after the dispersion the prepared suspension were passed to the proper area of the resist. The whole was stirred for 30 minutes in the furnace with a temperature of 70°C to let the ethanol completely evaporate. Then the resist was carefully removed and the material which did not adhere to the substrate was removed by means of compressed air. A ready system with four sensors is to be seen in Fig. 5, in which on the channels CH1-CH4: CH1-TiO₂ calcined at 350°C; CH2-TiO₂ calcined at 450°C; CH3-ZnO obtained in the synthesis type A, and CH4-ZnO obtained in the synthesis type B have been plotted, respectively.

The use of four-channel sensor matrix ensures simultaneous testing of four materials under identical conditions to ensure comparability of results.

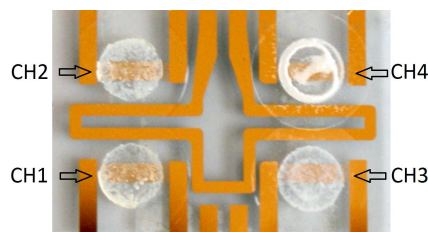


Fig. 5. Ready sensor made from nanoparticles on comb electrodes. CH1 – TiO₂ 350; CH2 – TiO₂ 450; CH3 – ZnO A; CH4 – ZnO B

5. Experimental details

The sensitivity of elaborated structures to the effect of NO₂ in synthetic was tested on the test-stand which was previously described in work [26]. In all these measurements the atmosphere was synthetic air (20% O₂ and 80% N₂). The tests were run at a continuous flow of synthetic air amounting to 500 ml/min.

The resistance of the respective transducer with a sensor layer was measured by means of the appliance AGILENT 34970 switch unit. Accuracy of used measurement card is $\pm 0.5 \cdot 10^{-4} \Omega$ for the range 10–100 Ω and $\pm 0.5 \cdot 10^{-3} \Omega$ for the range 100–999 Ω. Every single channel of sensor was connected to different channel of the card. It is to be admitted that the obtained structures are characterized a surprising low resistance of merely 15–200 Ω. It is entire resistance concerning both the sensor structure and the thin layer of gold, of which the transducers were made. The measurements were taken at a stabilized temperature of the substrate, rate of 115°C in order to eliminate the excess humidity from the sorptive surface and to aid the resorption of NO₂. Previously it had been attempted to perform these measurement at near room temperature (30°C). But at room temperature none of the transducers responded satisfactorily due to humidity and an entire lack of NO₂ resorption. The resistances of the transducers were measured at various concentrations of NO₂ within the range of 0–400 ppm. The cycle of measurements comprised an alternative introduction of pure synthetic air (by 30 minutes) and next a gaseous mixture concerning NO₂ in synthetic air (also by 30 minutes) into the measurement chamber, increasing successively the concentration of NO₂. The measurements were performed at two different values of humidity of air, viz. RH ≈ 5% (dry gas mixture) and RH ≈ 50% (humid gas mixture). The ambient temperature amounted to 23°C.

6. Investigations concerning the influence of NO₂ on sensor structures

As to be expected, the resistance of semiconductor sensors increases when the synthetic air contains NO₂ (Figs. 6 and 7). In reaction with the surface molecules this gas is subjected to chemisorption, which affects the number of charge carriers in the area adjacent to the surface. The growing resistance informs us that this sensor layer is getting impoverished in the amount of electrons, in resent of which the adsorbed gas molecules are forming traps localized in the forbidden band of semiconductor. As has already been mentioned, all the obtained structures display a surprising poor resistance; proba-

ably there dominates a mechanism of conduction through the surface states. The resistance of the produced materials is con-

tained within the range from about 15 to about 200 Ω on the distance between electrodes rate of 10 μm.

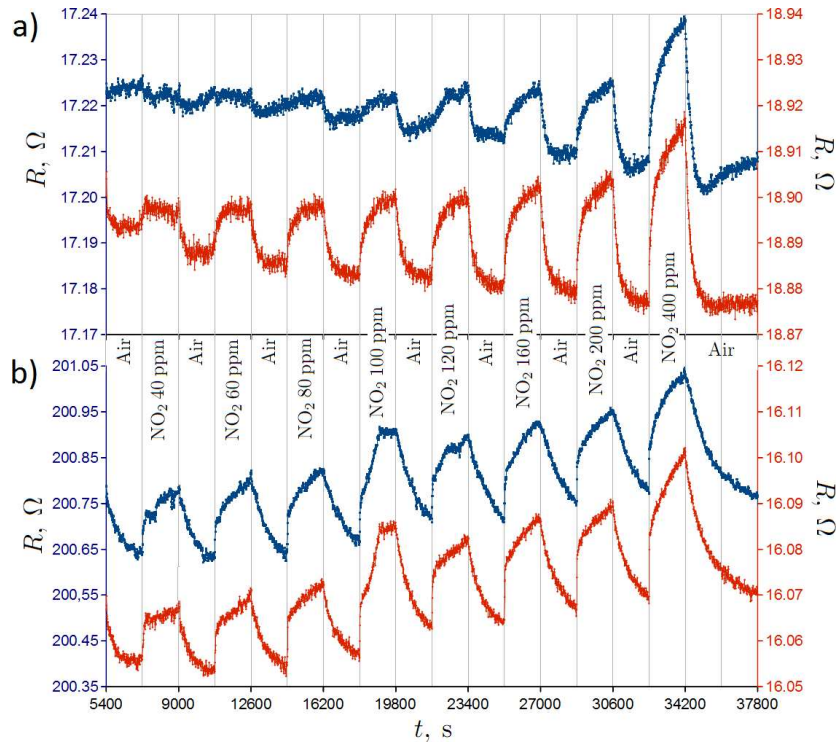


Fig. 6. Sensor response on NO₂ influence, T=115°C, humidity RH ≈ 5%. For: a) ZnO where blue and red plots represents data from structures obtained in synthesis A and B respectively; b) TiO₂ where blue and red plots represents data from structures obtained in calcination in 350°C and 450°C respectively

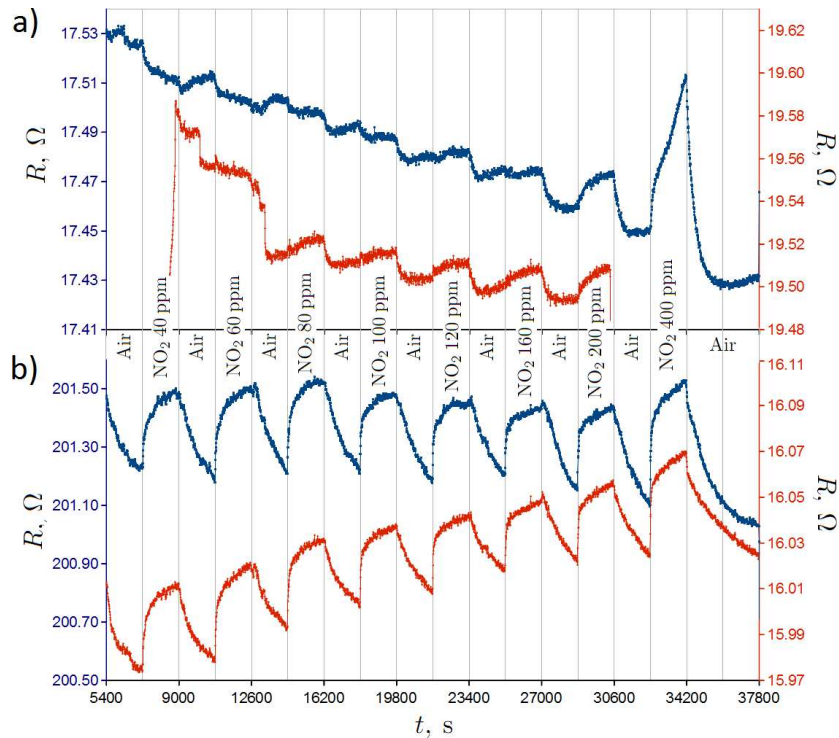


Fig. 7. Sensor response on NO₂ influence, T = 115°C, humidity RH ≈ 50%. For: a) ZnO where blue and red plots represents data from structures obtained in synthesis A and B respectively; b) TiO₂ where blue and red plots represents data from structures obtained in calcination in 350°C and 450°C respectively

6.1. ZnO structures. Basing on the results concerning ZnO structures (Fig. 6a) in a dry mixture ($RH \approx 5\%$), it is seen that in spite of considerably differing morphologies of the structures, the values of their resistance are approximately the same. It is, however, evident that various morphologies differ in their sensitivity to NO_2 .

In the case of ZnO from the synthesis B (Fig. 6A – red line) a reaction can be seen (perceptible due to the different level of noise) already at a concentration of 40 ppm NO_2 . In the case of ZnO – synthesis A (Fig. 6a – blue line) an increase of the resistance is to be observed only at a concentration of 100 ppm (not earlier). In the case of ZnO impregnates rather slowly, lagging even in 30 minutes. But, instead, a rapid drop of the resistance is to be observed after letting in fresh air. It should be mentioned that values of changes of the resistance depends in the case of ZnO structures on the concentration of NO_2 , which implies the possibility of scaling such a sensor and determining the actual concentrations. The sensor operates worse at a higher content of steam in the mixture amounting to $RH \approx 50\%$ (Fig. 7a). Then we witness a reduction of its sensitivity and encounter problems connected with its proper behavior. This becomes particularly evident in the case of ZnO – synthesis B (Fig. 7a – red line), where resistance jumps occur at concentrations of about 40 ppm and 200 ppm, probably due to the sedimentation of moisture in the pores of the material, which leads to a reduction of the resistance and changes in the impedance of the contacts. In the case of ZnO – synthesis A (Fig. 7a – blue line) the threshold of detect ability increased by a half in comparison with a dry mixture so sensitivity drops.

6.2. TiO_2 structures. The results concerning TiO_2 structures (Figs. 6b and 7b) show that in spite of their similar morphologies they display a different resistance depending on the temperature of calcinations. All the results obtained in the case of TiO_2 display a sufficient sensitivity to NO_2 already at a concentration of 40 ppm and justify the conclusion that the threshold of detection is below the tested range of concentrations. Nanoparticles of TiO_2 react promptly to the occurrence of NO_2 , and changes of the resistance differ in the entire considerably from the level of noise.

NO_2 is desorbed slowly, so that the sensor does not manage to desorb it entirely in the course of 30 minutes, which results in the fact that the resistance of the structure displays a slight tendency to increase during the time in which it is being measured (including of the characteristics). The sensitivity sensors based on TiO_2 layers is not interrogated by an elevated humidity (Fig. 7b). The response of the sensor in the case of humid mixture is even better than in the case of a dry one. When the mixture is dry, the values of changes in the resistance of the sensors depend on the concentration of NO_2 – sensor is scalable. Such dependence has not been observed in the case of dry mixtures, in which the sensor can't be scaled roughly for the purpose of determining adequately the concentration of NO_2 . A higher resistance and greater changes of the resistance can be observed in the case of nanorods and nanobelts of TiO_2 calcined at a temperature of $350^\circ C$.

7. Conclusions

The present paper proves that sensor structures of ZnO and TiO_2 react to slight concentrations of NO_2 already at $115^\circ C$. Such a low temperature contributes to a reduced consumption of energy by the sensors. The results of investigations indicate that TiO_2 is more sensitive to nitrogen dioxide both in a dry and a humid atmosphere. The sensoric properties of ZnO deteriorate when the gas mixture is moist, and the threshold of detection is twice worse. Humidity does not affect so much the sensitivity and threshold of detection of TiO_2 , but do not allow determining concretely the concentration of NO_2 . The influence of humidity on the operation of the sensors is a general problem in the technology of sensors. Attempts are being made to restrict this effect by applying dehumidifiers. The rate of the response of TiO_2 to the occurrence of NO_2 is shorter than that of ZnO. The latter is, however, characterized by a faster resorption. In the case of TiO_2 nanostructures the threshold of the detection of NO_2 is below the level of 40 ppm and may even lie lower the only a few ppm.

ZnO structures are characterized by a rapid desorption of NO_2 and may be applied for a quick disappearance detection of this gas. For this reason, array of sensors consisting of TiO_2 and ZnO permits to determine in a relatively short time both the moments of the occurrence and the fading of NO_2 in the gas mixture.

In the paper it has also been shown that the sensitivity of the sensors depended to a large extent on the morphology of the surface, which is particularly evident when the morphologies of ZnO differ considerably from each other.

It is to be stressed that the presented structures were pure semiconducting materials without any admixtures. By applying admixtures the sensoric properties can be still improved.

Acknowledgements. The work was partially sponsored by the National Centre for Scientific Researches and Development NCBiR within the grant OR00017912.

The participation of M.Sc. Marcin Procek was sponsored by means of the European Social Fund, comprised within the Project "SWIFT" POKL. 08.02.01-24-005/10.

M.Sc. Sabina Drewniak was awarded a scholarship within the frame of DoktorRIS on behave of the innovations of Silesia, financed jointly with the European Union Social Found.

REFERENCES

- [1] S. Zampolli, I. Elmi, J. Stürmann, S. Nicoletti, L. Dori, and G.C. Cardinali, "Selectivity enhancement of metal oxide gas sensors using a micromachined gas chromatographic column", *Sensors and Actuators B: Chemical* 105 (2), 400–406 (2005).
- [2] D.D. Lee and D.K. Lee, "Environmental gas sensors", *IEEE Sensors J.* 1, 214–224 (2001).
- [3] D.L. Wang, A.T. Chen, Q.F. Zhang, and G.Z. Cao, "Room-temperature chemiresistive effect of TiO_2 nanowires to nitroaromatic and nitroamine explosives", *IEEE Sensors J.* 11 (6), 1352–1358 (2011).
- [4] Z. Bielecki, J. Janucki, A. Kawalec, J. Mikolajczyk, N. Palka, M. Pasternak, T. Pustelny, T. Steciewicz, and J. Wojtas, "Sensors and systems for the detection of explosive devices – an overview", *Metrol. Meas. Syst.* 19 (1), 3–28 (2012).

- [5] A. Murugarajan, G.L. Samuel, "Measurement modeling and evaluation of surface parameter using capacitive-sensor based measurement system", *Metrol. Meas. Syst.* XVIII (3), 403–418 (2011).
- [6] M. Kastek, T. Piątkowski, and P. Trzaskawka, "Infrared imaging Fourier transform spectrometer as the stand-off gas detection system", *Metrol. Meas. Syst.* 18 (4), 607–620 (2011).
- [7] Y.X. Yu and D.S. Xu, "Single-crystalline TiO₂ nanorods: highly active and easily recycled photocatalysts", *Applied Catalysis B: Environmental* 73 (1–2), 166–171 (2007).
- [8] W. Zeng and T.M. Liu, "Gas-sensing properties of SnO₂-TiO₂-based sensor for volatile organic compound gas and its sensing mechanism", *Physica B: Condensed Matter* 405 (5), 1345–1348 (2010).
- [9] L. You, Y.F. Sun, J. Ma, and Y. Guan, "Highly sensitive NO₂ sensor based on square-like tungsten oxide prepared with hydrothermal treatment", *Sensors and Actuators B: Chemical* 157 (2), 401–407 (2011).
- [10] W.W. Guo, T.M. Liu, and L. Huang, "Gas-sensing property improvement of ZnO by hierarchical flower-like architectures", *Materials Letters* 65 (23–24), 3384–3387 (2011).
- [11] T. Pustelny, E. Maciak, Z. Opilski, A. Piotrowska, E. Papis, and K. Golaszewska, "Investigation of ZnO sensing structure on NH₃ action by means of the surface plasmon resonance method", *Eur. Physical J: Special Topics* 154 (1), 165–170 (2008).
- [12] W. Jakubik, M. Urbanczyk, E. Maciak, and T. Pustelny, "Surface acoustic wave hydrogen gas sensor based on layered structure of palladium/meta-free phthalocyanine", *Bull. Pol. Ac.: Tech.* 56 (2) 133–138 (2008).
- [13] P. Struk, T. Pustelny, K. Golaszewska, E. Kamińska, M. Borysewicz, M. Ekielski, and A. Piotrowska, "Photonic structures with grating couplers based on ZnO", *Opto-electron. Rev.* 19 (4), 462–467 (2011).
- [14] T. Pustelny, E. Maciak, Z. Opilski, and M. Bednorz, "Optical interferometric structures for application in gas sensors", *Optica Applicata* 37 (1–2) 187–194 (2007).
- [15] B. Pustelny and T. Pustelny, "Transverse acoustoelectric effect applying in surface study of GaP:Te(111)", *Acta Physica Polonica A* 116 (3), 385–388 (2009).
- [16] H. Chen, Y. Liu, C. Xie, J. Wu, D. Zeng, and Y. Liao, "A comparative study on UV light activated porous TiO₂ and ZnO ?lm sensors for gas sensing at room temperature", *Ceramics Int.* 38, 503–509 (2012).
- [17] M. Gong, Y.H. Li, Z.H. Hu, and Z. Zhou, "Ultrasensitive NH₃ gas sensor from polyaniline nanograin enshased TiO₂ fibers", *J. Physical Chemistry C* 114, 9970–9974 (2010).
- [18] G.S. Devi and T. Hyodo, and Y. Shimizu, "Synthesis of mesoporous TiO₂-based powders and their gas-sensing properties", *Sensors and Actuators, B: Chemical* 87, 122–136 (2002).
- [19] C.M. Carney, S.H. Yoo, and S.A. Akbar, "TiO₂-SnO₂ nanostructures and their H₂ sensing behavior", *Sensors and Actuators, B: Chemical* 29, 108–122 (2005).
- [20] E.D. Gaspera, M. Guglielmi, and S. Agnoli, "Au nanoparticles in nanocrystalline TiO₂-NiO films for SPR-based, selective H₂S gas sensing", *Chemistry of Materials* 22, 3407–3417 (2010).
- [21] D. Barreca, G. Carraro, and E. Comini, "Novel synthesis and gas sensing performances of CuO-TiO₂ nanocomposites functionalized with Au nanoparticles", *J. Physical Chemistry C* 115, 10510–10517 (2011).
- [22] L. Gu, K. Zheng, Y. Zhou, J. Li, X. Mo, G.R. Patzke, and G. Chen, "Humidity sensors based on ZnO/TiO₂ core/shell nanorod arrays with enhanced sensitivity", *Sensors and Actuators, B: Chemical* 159 (1), 1–7 (2011).
- [23] T. Pisarkiewicz, T. Kenig, A. Radosz, and W. Maziarz, "Solution growth of ZnO sub-micro rods enhanced by electric field", *Bull. Pol. Ac.: Tech.* 59 (4), 425–428 (2011).
- [24] L. Huang, T. Liu, H. Zhang, W. Guo, and W. Zeng, "Hydrothermal synthesis of different TiO₂ nanostructures: structure, growth and gas sensor properties", *J. Materials Science: Materials in Electronics* 23, 1–6 (2012).
- [25] S. Balaji, Y. Djaoued, J. Robichaud, "Phonon confinement studies in nanocrystalline anatase-TiO₂ thin films by micro Raman spectroscopy", *J. Raman Spectroscopy* 37 (12), 1416–1422 (2006).
- [26] M. Urbańczyk, E. Maciak, K. Gut, T. Pustelny, and W. Jakubik, "Layered thin film nanostructures of Pd/WO_{3-x} as resistance gas sensors", *Bull. Pol. Ac.: Tech.* 59 (4), 401–406 (2011).